

## Chapter 5

# Reductive Defluorination of Aqueous Perfluorinated Alkyl Surfactants: Effects of Ionic Headgroup and Chain Length

Sections reprinted with permission from Park, H.; Vecitis, C. D.; Cheng, J.; Choi, W.; Mader, B. T.; Hoffmann, M. R. *Journal of Physical Chemistry A* **2009**, *113*, 4, 690–696.  
© 2009 American Chemical Society.

## Abstract

Perfluorinated chemicals (PFCs) are distributed throughout the environment. In the case of perfluorinated alkyl carboxylates and sulfonates, they can be classified as persistent organic pollutants since they have relatively high water solubilities and are resistant to oxidation. With this in mind, we report on the reductive defluorination of perfluorobutanoate, PFBA ( $\text{C}_3\text{F}_7\text{CO}_2^-$ ), perfluorohexanoate, PFHA ( $\text{C}_5\text{F}_{11}\text{CO}_2^-$ ), perfluorooctanoate, PFOA ( $\text{C}_7\text{F}_{15}\text{CO}_2^-$ ), perfluorobutane sulfonate, PFBS ( $\text{C}_4\text{F}_9\text{SO}_3^-$ ), perfluorohexane sulfonate, PFHS ( $\text{C}_6\text{F}_{13}\text{SO}_3^-$ ), and perfluorooctane sulfonate, PFOS ( $\text{C}_8\text{F}_{17}\text{SO}_3^-$ ), by aquated electrons,  $e_{\text{aq}}^-$ , that are generated from the UV photolysis ( $\lambda = 254 \text{ nm}$ ) of iodide. The ionic headgroup ( $-\text{SO}_3^-$  vs.  $-\text{CO}_2^-$ ) has a significant effect on the reduction kinetics and extent of defluorination (F-Index;  $-\text{[F]}^-_{\text{produced}}/[\text{PFC}]_{\text{degraded}}$ ). Perfluoroalkylsulfonate reduction kinetics and the F-index increase linearly with increasing chain length. In contrast, perfluoroalkylcarboxylate chain length appears to have a negligible effect on the observed kinetics and the F-index. H/F ratios in the gaseous fluoroorganic products are consistent with measured F-indexes. Incomplete defluorination of the gaseous products suggests a reductive cleavage of the ionic headgroup occurs before complete defluorination. Detailed mechanisms involving initiation by aquated electrons are proposed.

## Introduction

Fluorinated chemicals (FCs), such as fluorotelomer alcohols, partially fluorinated amphiphiles, perfluoroalkyl carboxylates, and perfluoroalkylsulfonates, have been widely used for water-proofing textiles, as protective coatings on metals, in aqueous film-forming foams (AFFFs), in semi-conductor etching, and as lubricants. Atmospheric oxidation<sup>1,2</sup> and bio-transformation<sup>3,4</sup> can convert partially fluorinated chemicals into environmentally persistent perfluorochemicals (PFCs). For example, perfluorooctane sulfonate (PFOS) and perfluorooctanoate (PFOA) have been detected globally in surface waters<sup>5,6</sup> due to atmospheric<sup>7</sup> and oceanic transportation<sup>8</sup>.

Perfluorochemicals are chemically inert due to relatively high organic bond strengths (e.g., 413.0 kJ/mol for  $\text{F}_3\text{C}-\text{CF}_3$ ; 530.5 kJ/mol for  $\text{F}-\text{C}_2\text{F}_5$ )<sup>9</sup> and fluorine's electronegativity making them resistant to conventional advanced oxidation processes (AOPs)<sup>10-13</sup>. For example, hydroxyl radical ( $\bullet\text{OH}$ ) with a reduction potential of  $E^\circ = 2.73 \text{ V}^{14}$  reacts with a typical hydrocarbon octanoate with a second-order rate constant that is  $>10^9 \text{ M}^{-1}\text{s}^{-1}$ <sup>15</sup>, however, the corresponding second-order rate constants, when the compounds are perfluorinated, have an upper limit of  $< 10^5 \text{ M}^{-1}\text{s}^{-1}$  (e.g., PFOA and PFOS)<sup>16</sup>. Direct electron transfer oxidation processes (e.g.,  $\text{S}_2\text{O}_8^{2-}/\text{UV}^{13}$  and  $\text{PW}_{12}\text{O}_{40}^{3-}/\text{UV}^{12}$ ) and aqueous pyrolysis (i.e., sonolysis)<sup>17,18</sup> have shown to be more effective for PFC remediation. Perfluorocarboxylate reaction rate constants with sulfate radical ( $\text{SO}_4^{\bullet-}$ ) are estimated to be on the order of  $10^4 \text{ M}^{-1}\text{s}^{-1}$ <sup>19,20</sup>. At this level, the reaction rate constants are orders of magnitude lower than the sulfate radical constants with hydrocarbons<sup>21</sup>.

Reductive remediation of perfluorocarboxylates and perfluorosulfonates is feasible<sup>22–24</sup>. For example, PFOS and PFHS can be reduced by elemental iron (Fe(0),  $E = -0.447$  V)<sup>14</sup> in water under extreme conditions (350 °C, 20 MPa)<sup>23,24</sup>. Aromatic<sup>25,26</sup>, benzylic<sup>27</sup>, olefinic<sup>28,29</sup>, and tertiary<sup>30–32</sup> fluoroorganics readily undergo reductive defluorination by chemical and electrochemical methods. Studies on linear fluorochemicals containing only secondary<sup>20</sup> and primary<sup>33</sup> C-F bonds are limited due to low ( $E < -2.7$  V) reduction potentials<sup>34,35</sup>. Reductive fluoride elimination is influenced by a number of chemical properties, such as C-F bonding character (e.g.,  $\sigma$  vs.  $\pi$  character)<sup>26</sup>, electron density<sup>36</sup>, redox potential<sup>35</sup>, anion radical stability<sup>25</sup>, ionic head group<sup>16</sup>,  $-(CF_2)_n-$  chain length<sup>20</sup>, and electron-donating reagent strength<sup>37</sup>. The activation energies of aqueous electron reactions with halo-organics are invariable and small (6 to 30 kJ/mol) due to tunneling effects<sup>38</sup>. However, fluoroorganic reduction rates are lower than other organohalogens since fluorine has no low-lying vacant d-orbital to accept an electron. Low PFC water solubility has limited most reductive defluorination studies to organic solvents<sup>39</sup>.

A systematic study on the reductive remediation of aqueous PFCs ( $C_3F_7CO_2^-$ ,  $C_5F_{11}CO_2^-$ ,  $C_7F_{15}CO_2^-$ ,  $C_4F_9SO_3^-$ ,  $C_6F_{13}SO_3^-$ , and  $C_8F_{17}SO_3^-$ ) has yet to be completed. We here utilize the aquated electron ( $e_{aq}^-$ ,  $E^\circ_{aq/e} = -2.9$  V), a powerful reductant, to decompose a number of perfluoroalkyl carboxylates and perfluoroalkyl sulfonates of varying chain (hydrophobic tail) length (e.g., C3 to C8). Aquated electrons are generated from UV-photolysis of aqueous iodide solutions via charge-transfer-to-solvent (CTTS) states<sup>40</sup>. The kinetics and mechanism of aqueous PFC reduction is significantly affected by ionic headgroup speciation and fluorinated tail length.

## Experimental Details

Perfluorooctanoate (PFOA:  $\text{C}_7\text{F}_{15}\text{CO}_2\text{NH}_4$ , 3M), perfluorohexanoate (PFHA:  $\text{C}_5\text{F}_{11}\text{CO}_2\text{H}$ , > 97%, Fluka), perfluorobutanoate (PFBA:  $\text{C}_3\text{F}_7\text{CO}_2\text{H}$ , > 98%, Aldrich), perfluorooctane sulfonate (PFOS:  $\text{C}_8\text{F}_{17}\text{SO}_3\text{K}$ , 3M), perfluorohexane sulfonate (PFHS:  $\text{C}_6\text{F}_{13}\text{SO}_3\text{K}$ , > 98%, Fluka), and perfluorobutane sulfonate (PFBS:  $\text{C}_4\text{F}_9\text{SO}_3\text{K}$ , 3M Company) were used as received. PFC stock solutions were prepared to be 500 mg/L and the pH was adjusted to between 6 and 8 with HCl or  $\text{NH}_4\text{OH}$ . A 1 mol/L KI (Fisher) aqueous stock solution was freshly prepared every week and stored in the dark.

PFC and KI stock solutions were diluted with Milli-Q water to 30 mL. Photolysis was completed in a Pyrex glass reactor with a quartz window and irradiated with 254 nm light source (UVP, 8 W). Argon or air was continuously purged through the aqueous solution or through the headspace. A 0.5 mL sample aliquot was taken at different time points during photolysis, and if necessary, diluted prior to analysis. The incident photon flux was determined to be  $5.17(\pm 0.06) \times 10^{-5} \text{ mol L}^{-1} \text{ min}^{-1}$  by iodide/iodate actinometry using the intrinsic quantum yield of iodide/iodate as a reference<sup>38</sup>.

Initial PFC and possible aqueous-phase intermediate analysis was completed by HPLC-MS (Agilent 1100 LC and Agilent Ion Trap) with a Betasil C18 column (Thermo-Electron) of dimensions 2.1 mm ID, 100 mm length and 5  $\mu\text{m}$ -particle size. A 2 mM aqueous ammonium acetate:methanol gradient mobile phase at a flow rate of 0.3 mL min<sup>-1</sup> was used for separation. The samples were analyzed by the MS/MS (Agilent, MSD Trap) in negative mode monitoring for the molecular ions of PFOS ( $m/z = 499$ ), PFHS ( $m/z = 399$ ), and PFBS ( $m/z = 299$ ), and decarboxylated ions of PFOA ( $m/z = 369$ ), PFHA ( $m/z = 269$ ), and PFBA ( $m/z = 169$ ). The nebulizer gas pressure was 40 PSI, drying gas flow rate and temperature were 9 L min<sup>-1</sup> and 325 °C, the capillary voltage

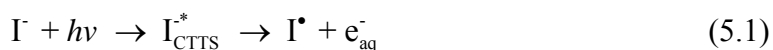
was set at + 3500 V and the skimmer voltage was – 15 V. HPLC analytical procedures are detailed elsewhere<sup>18</sup>.

Ion chromatography (Dionex DX-500) was used for the analysis of fluoride and other ionic intermediates. 0.5 mL aliquots were transferred from the reactor to disposable PolyVial sample vials (PolyVial) and sealed with filter caps (PolyVial) and loaded onto an AS-40 autosampler. The 0.5 ml sample was injected and anions were separated on an IonPac AS11-HC anion exchange column and quantified by conductivity measurement.

The gaseous fluorointermediates produced were analyzed by GC-MS. The reactor headspace was continuously purged with argon. The purge gas containing the reaction intermediates was circulated over a thermal desorption tube (CarboTrap, Supelco) to adsorb the intermediates. After completion of the reaction, the purge gas was turned off and the tubes were sealed to atmosphere. GC-MS analysis consisted of thermal desorption of the intermediates from the tube (OI Analytical), and analysis of the desorbed gases by GC-MS (Agilent 6890 GC and 5973 MSD).

## Results and Discussion

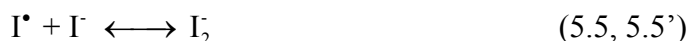
Figure 5.1 shows the time course for the reductive decomposition of PFOS and PFOA during the photolysis ( $\lambda = 254$  nm) of an aqueous iodide solution in the presence of argon and air ( $[\text{PFOS}]_i = 0.20 \mu\text{M}$ ,  $[\text{PFOA}]_i = 0.24 \mu\text{M}$ ,  $[\text{I}^-]_i = 10 \text{ mM}$ ). The quantum yield for the generation of aquated electrons from iodide photolysis at 248 nm (eq. 5.1) is 28%<sup>39</sup>. In the presence of air, PFOS and PFOA are degraded (Figure 5.1) due to the rapid reaction ( $k_3 = 1.9 \times 10^{10} \text{ M}^{-1} \text{ s}^{-1}$ )<sup>15</sup> of the aquated electron with dissolved oxygen ( $\sim 0.2 \text{ mM}$ ) (eq. 5.3).



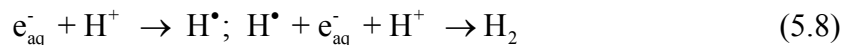


However, in the presence of Ar (i.e., in the absence of air) PFOS and PFOA initial decomposition (eq. 5.4, where X = S and A for sulfonate and carboxylate, respectively) follows pseudo-first-order kinetics. Under these conditions, the rate of PFOS reduction is two times greater than that of PFOA ( $k_{app}^{-PFOS} = 6.5 \times 10^{-3} \text{ min}^{-1}$ ;  $k_{app}^{-PFOA} = 2.9 \times 10^{-3} \text{ min}^{-1}$ ). The relative photoreduction rates ( $k_{app}^{-PFOS} / k_{app}^{-PFOA}$ ) are consistent with those observed in pulse radiolysis<sup>16</sup> where  $k_4^{-PFOS}$  and  $k_4^{-PFOA}$  for reduction by aquated electrons are reported to be  $7.3 \times 10^7 \text{ M}^{-1} \text{ s}^{-1}$  and  $5.1 \times 10^7 \text{ M}^{-1} \text{ s}^{-1}$ , respectively. A more recent laser flash photolysis study<sup>20</sup> reported  $k_4^{-PFOA} = 1.7 \times 10^7 \text{ M}^{-1} \text{ s}^{-1}$ .

The quantum yields for the photoreduction of PFOS and PFOA are  $11.8 \times 10^{-4}$  and  $6.4 \times 10^{-4}$ , respectively. The relatively low quantum yields ( $\sim 0.1\%$ ) indicate that there are quenching reactions for aquated electrons. Photodetachment of an aquated electron produces iodine atom ( $I^\bullet$ , eq. 5.1).  $I^\bullet$  complexes with a neighboring iodide forming the diiodide radical anion ( $I_2^-$ , eq. 5.5') with an equilibrium constant,  $K_5 > 1.2 \times 10^4$ . The complexation is diffusion controlled and  $[I]_{ss} \gg [e^-]_{ss}$  such that  $k_5 \gg k_2$  and  $I_2^-/I^\bullet = 120$ . The diffusion-controlled reaction ( $k_6 = 3.2 \times 10^9 \text{ M}^{-1} \text{ s}^{-1}$ ) between two  $I_2^-$  molecules (eq. 5.6) produces triiodide ( $I_3^-$ ) and  $I^-$ .

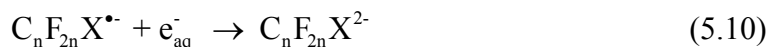
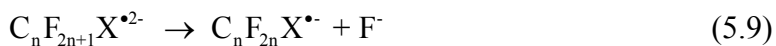


Aquated electron quenching may occur via  $I^\bullet$  carriers (eq. 5.7) or by way of hydrogen production (eq. 5.8).

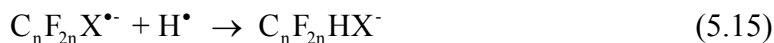
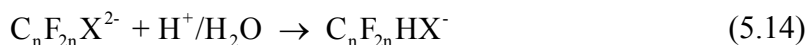
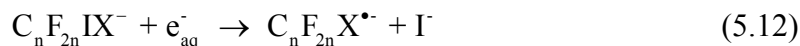


As shown in Figure 5.2a, the steady-state triiodide concentration,  $[I_3^-]_{ss}$ , is almost negligible in aqueous solutions without PFOX (i.e., in the absence of dissolved oxygen) and increases to micromolar levels upon addition of PFOX, suggesting the  $I^\bullet$  carrier quenching is the predominant mechanism. Minimal pH changes during the reactions (Figure 5.2b) is consistent with  $I^\bullet$  carrier quenching.  $H^\bullet$ , intermediates in eq. 5.8, may also be quenched by  $I^\bullet$  carriers. In particular in the absence of PFOX and oxygen, pH rises up to 10–11 immediately after light irradiation, probably due to proton consumption by  $e_{aq}^-$  (eq. 5.8). The PFOA photolysis also continuously increases the pH, whereas the pH at the PFOS photolysis is decreased soon after initial increase. The bell-shaped pH change is ascribed to the initial proton consumption and the post-release of fluoride ion (i.e.,  $pK_a(HF) = 3.45$ ). This indicates that the pH changes are primarily caused by the fluoride production and could be used as an indicator of the defluorination.

Reaction of the initial perfluorinated alkyl carboxylate or sulfonate with  $e_{aq}^-$  yields the corresponding radical anion ( $C_nF_{2n+1}X^{\bullet 2-}$ ;  $n = 8$ ,  $X = SO_3$  for PFOS $^{\bullet 2-}$ ;  $n = 7$ ,  $X = CO_2$  for PFOA $^{\bullet 2-}$ , eq. 5.4). The radical anion will quickly decompose via fluoride elimination<sup>27,41</sup> to yield the perfluoroalkyl radical ( $C_nF_{2n}X^\bullet$ , eq. 5.9).







The electrophilic perfluoroalkyl radicals<sup>42-44</sup> may react further with  $e_{\text{aq}}^-$  to yield carbanions ( $\text{C}_n\text{F}_{2n}\text{X}^{2-}$ , eq 10) or with  $\text{I}^{\bullet}$  carriers (i.e.,  $\text{I}^{\bullet}$ ,  $\text{I}_2^{\bullet-}$ ,  $\text{I}_3^{\bullet-}$ ) to yield the perfluoroalkyl iodide carboxylate or sulfonate ( $\text{C}_n\text{F}_{2n}\text{IX}^-$ , eq. 5.11). The perfluoroalkyl iodide carboxylates and sulfonates will be converted back to perfluoroalkyl radicals via photolytic homolysis of the C-I bond (eq 5.11') or via reaction with  $e_{\text{aq}}^-$  to yield the radical and  $\text{I}^-$  (eq. 5.12)<sup>45</sup>. In organic solvents, the carbanion intramolecularly defluorinates to give an olefin (eq 5.13).<sup>27,35</sup> However, in the presence of water, the carbanion, which is a strong base, will be protonated. An overall H/F exchange may also occur via reaction of a fluoroalkyl radical anion ( $\text{C}_n\text{F}_{2n}\text{X}^{\bullet-}$ ) with an  $\text{H}^{\bullet}$  (eq. 5.15). If an H/F exchange product retains the anionic carboxylate or sulfonate terminal group, it will remain in the aqueous phase and proceed through sequential H/F exchanges. Subsequent  $e_{\text{aq}}^-$  reductions with partially defluorinated intermediates ( $\text{C}_n\text{F}_{2n}\text{IX}^-$ ,  $\text{C}_n\text{F}_{2n-1}\text{X}^-$  or  $\text{C}_n\text{F}_{2n}\text{HX}^-$ ) should be faster than the initial defluorination step<sup>27</sup>.

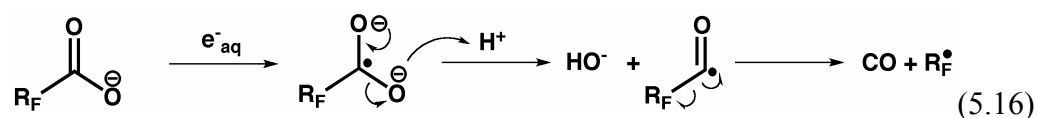
A systematic study of perfluorochemical decomposition was completed by reducing the shorter-chained PFCs (PFHS, PFBS, PFHA, and PFBA, where H = hexane and B = butane) under the same photolytic conditions. Figure 5.3a and b show the time-dependent reactions of all six PFCs with the aquated electron. The three perfluoroalkyl carboxylates

have similar pseudo-first-order degradation rates,  $k_{app}^{-PFOA} \approx k_{app}^{-PFHA} \approx k_{app}^{-PFBA} \approx 1.3 \times 10^{-3} \text{ min}^{-1}$  (Figure 5.3a), and the carboxylate kinetics are plotted on the sulfonate curve as a dashed line for comparison (Figure 5.3b). In contrast, the perfluoroalkyl sulfonates kinetics are dependent on chain length,  $k_{app}^{-PFOS} > k_{app}^{-PFHS} > k_{app}^{-PFBS}$  and the rate decreases with decreasing chain length ( $3.0 \times 10^{-3}$ ,  $1.2 \times 10^{-3}$ , and  $4.0 \times 10^{-4} \text{ min}^{-1}$  for PFOS, PFHS, and PFBS, respectively). Accordingly, quantum yields for the degradation of the carboxylates are independent of chain length, i.e., PFBA ( $7.05 \times 10^{-4}$ )  $\approx$  PFHA ( $6.94 \times 10^{-4}$ )  $\approx$  PFOA ( $6.36 \times 10^{-4}$ ), whereas those for the sulfonates are chain length dependent, i.e., PFOS ( $11.8 \times 10^{-4}$ )  $>$  PFHS ( $5.71 \times 10^{-4}$ )  $>$  PFBS ( $2.41 \times 10^{-4}$ ) (Table 5.1).

The aqueous electron-mediated reduction of perfluorochemicals eventually eliminates fluoride ( $\text{F}^-$ ) and thus fluoride measurements give insight into the overall mechanism and extent of reduction. The time-dependent  $\text{F}^-$  production during degradation of the perfluorocarboxylates and the perfluorosulfonates are shown in Figures 5.4a and b, respectively. Similar to the decomposition kinetics, the perfluorocarboxylate  $\text{F}^-$  production has no chain-length dependence ( $[\text{F}^-] = 5 \sim 12 \text{ } \mu\text{M}$  at 2.5 h-photolysis), whereas the perfluorosulfonate  $\text{F}^-$  production is dependent on chain length;  $\text{F}^-$  production decreases with decreasing chain length ( $[\text{F}^-] = 58, 23$ , and  $5 \text{ } \mu\text{M}$  at 2.5 h-photolysis for PFOS, PFHS, and PFBS, respectively). Alternatively, the  $\text{F}^-$  yield can be evaluated using the *F-index* (i.e.,  $-\text{[F}^-]_{\text{produced}}/\text{[PFC]}_{\text{degraded}}$ ). F-indices for all PFCs are observed to grow linearly over the course of the reaction. For the three carboxylates, the F-index is between 1 and 2, suggesting a reductive mechanism independent of chain length. For the sulfonates, the F-index is related to the number of carbons in the hydrophobic tail, with approximately one defluorination per carbon (i.e., 9, 6, and 3 for PFOS, PFHS, and PFBS,

respectively). In both cases, defluorination is incomplete, suggesting loss of partially defluorinated species to the gas phase, which implies loss of the sulfonate or carboxylate ionic headgroup prior to complete defluorination.

The data from Figures 5.3 and 5.4 has been compiled in Figure 5.5.  $k_{app}^{-PFC}$ , and the F-index for all six PFCs are plotted as a function of fluorocarbon chain length. It appears that the carboxylates have a similar degradation mechanism since both the kinetics and F-indices show no chain-length dependence. Minimal defluorination suggests that the carboxylate group is lost shortly after the initial reduction or simultaneously with the reduction. In the case of hydrocarbon carboxylates,<sup>46</sup> the aquated electron-mediated reduction occurs at the carbonyl group with subsequent loss of  $\text{HO}^-$  and  $\text{CO}$ , yielding an alkyl radical, or in this case a fluoroalkyl radical ( $\text{R}_\text{F}\bullet$ , eq. 5.16).

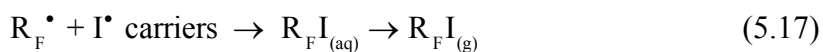


An initial defluorination may be required at the alpha carbon to the carbonyl to favor the decarboxylation mechanism. A similar mechanism may be active for the desulfonation of the perfluoroalkyl sulfonates. In contrast to the carboxylates, a larger number of reductive defluorinations is required prior to loss of the ionic headgroup, suggesting initial defluorination occurs at carbons away from the sulfonate group.

Gaseous intermediates produced during PFC reduction were trapped in thermal desorption tubes and analyzed by GC-MS. A number of intermediates were identified, which were composed of carbon, fluorine, hydrogen, and iodine (Figure 5.6 and Table 5.2). The perfluoroalkyl carboxylate gaseous intermediates were primarily composed of C-F bonds, consistent with F-indices. The perfluoroalkyl sulfonate intermediates had a

greater degree of H/F exchange (i.e., degree of reduction), which is also consistent with F-indices for these compounds. The agreement between H/F exchange and the F-index suggests initial defluorination is primarily followed by protonation of the carbanion intermediate (eq. 5.14) or perfluororadical reaction with H-atom (eq. 5.15), with minor olefinization (eq. 5.13). It is of note that the reduction products of the perfluorinated chemicals in aprotic solvents are primarily olefins. Also, the sulfonates have a larger number of unique gaseous intermediates as compared to the carboxylates. For example, PFOS has a more diverse set of intermediates ranging from C<sub>1</sub> to C<sub>8</sub> and 3 times the total number of intermediates as PFOA (Table 5.2).

A large majority of the gases produced are iodinated and the noniodinated minority generally contains an olefin. On average, a single I<sup>•</sup> is incorporated into a gaseous fluorointermediate suggesting partitioning out of solution quickly follows neutral fluororadical iodination. For example, the reaction of the fluoroalkyl radical (R<sub>F</sub>•) produced in eq. 5.16 with I<sup>•</sup> results in a product that has a high tendency to partition into the vapor phase (eq. 5.17).



The absence of vapor-phase intermediates with higher degrees of iodination may be due to subsequent photolytic cleavage or reduction of C-I bonds by aquated electron (eqs. 5.11' and 5.12, respectively) formed from the aqueous fluoro-intermediates. It should be noted that a C-I bond (bond strength, 209 kJ/mol) is weaker than a C-F bond (bond strength, 460 kJ/mol). In addition, perfluorooctyl iodide (C<sub>8</sub>F<sub>17</sub>I) is observed as the heaviest intermediate during PFOS photolysis, whereas perfluorohexyl iodide (C<sub>6</sub>F<sub>13</sub>I)—*not* C<sub>7</sub>F<sub>15</sub>I—is detected during PFOA photolysis. This suggests the presence of a

transient perfluorooctyl radical ( $\text{C}_8\text{F}_{17}\bullet$ ) intermediate during PFOS photolysis and perfluorohexyl radical ( $\text{C}_6\text{F}_{13}\bullet$ ) generated from PFOA photolysis (eq. 5.17). The sulfonate elimination from an intact fluorocarbon tail is also observed during PFHS photolytic reduction (e.g.,  $\text{C}_6\text{F}_{13}\text{I}$ ,  $\text{C}_6\text{F}_{12}\text{HI}$ ) and PFBS reduction (e.g.,  $\text{C}_4\text{F}_4\text{H}_4$ ). In addition, the loss of the carboxylate group plus a tail carbon is observed during PFHA photolysis (e.g.,  $\text{C}_4\text{F}_9\text{I}$ ). However, in the case of PFBA, a  $\text{C}_3$  intermediate is detected, likely due to the altered properties as the  $\text{CF}_2\text{-CF}_2$  chain length shortens.

In summary, the ionic head group, carboxylate vs. sulfonate, has a significant effect on the kinetics and mechanism of perfluoroalkyl surfactant reduction by aqueous electrons. The fluorocarbon tail length of the perfluorinated alkyl sulfonates significantly affects the reduction rate and extent of defluorination, implying the existence of multiple reaction sites across the fluorocarbon tail. In contrast, perfluorinated alkyl carboxylates have invariable reaction rates with aqueous electrons and similar degrees of defluorination implying a similar initial reaction site near the ionic headgroup. Ionic headgroup cleavage and loss of the subsequent neutral to the gas phase is likely cause of incomplete defluorination. Detailed studies utilizing a more quantitative intermediate analysis to better understand defluorination kinetics and mechanism are being investigated.

## Figures

**Figure 5.1.** Pseudo-first-order plots of PFOX UV<sub>254 nm</sub> KI photolysis. Irradiation of an aqueous KI-PFOX solution in the presence and absence of oxygen (i.e., air vs. Ar). PFOS and PFOA are identically 100 ppb, i.e.,  $[\text{PFOA}]_0 = 0.24 \mu\text{M}$ ;  $[\text{PFOS}]_0 = 0.20 \mu\text{M}$ ; and  $[\text{KI}]_0 = 10 \text{ mM}$

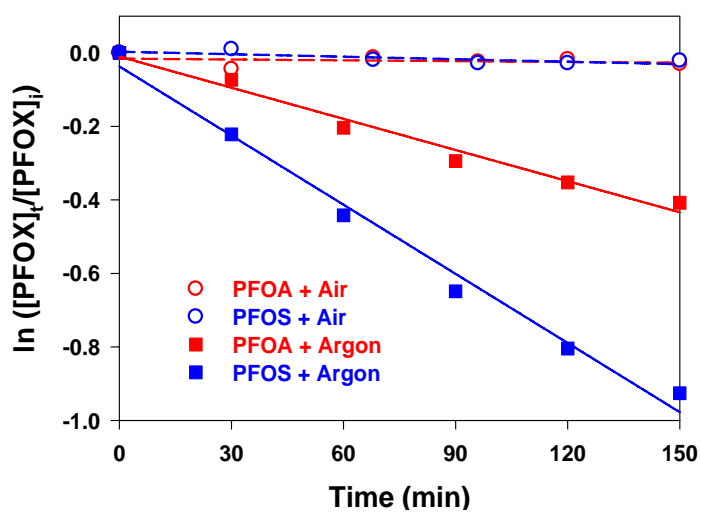


**Figure 5.2.**  $I_3^-$  production and pH change during PFOX UV-KI photolysis. A) triiodide production, and B) pH change during the photolysis of aqueous iodide-PFOX solutions.

$[PFOS]_0 = 20 \mu M$ ;  $[PFOA]_0 = 24 \mu M$ ;  $[KI]_0 = 10 \text{ mM}$ ;  $\lambda = 254 \text{ nm}$  and in the presence of

Ar

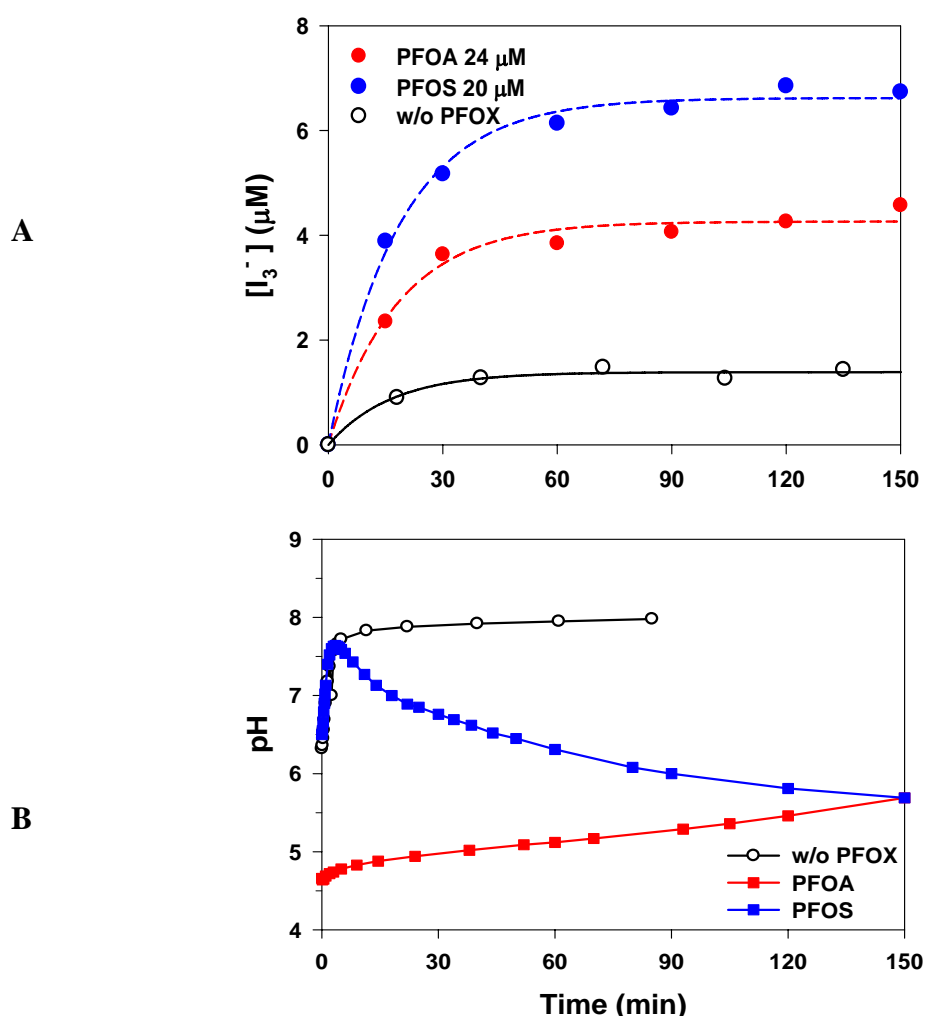


**Figure 5.3.** PFXA and PFXS (X = O, H, B) degradation during UV-KI photolysis.  $\lambda = 254$  nm irradiation of aqueous KI solution in the presence of Ar. All PFCs are identically 10 ppm, i.e.,  $[\text{PFOS}]_0 = 20 \mu\text{M}$ ;  $[\text{PFHS}]_0 = 25.1 \mu\text{M}$ ;  $[\text{PFBS}]_0 = 33.4 \mu\text{M}$ ;  $[\text{PFOA}]_0 = 24 \mu\text{M}$ ;  $[\text{PFHA}]_0 = 31.9 \mu\text{M}$ ;  $[\text{PFBA}]_0 = 46.0 \mu\text{M}$ ; and  $[\text{KI}]_0 = 10 \text{ mM}$

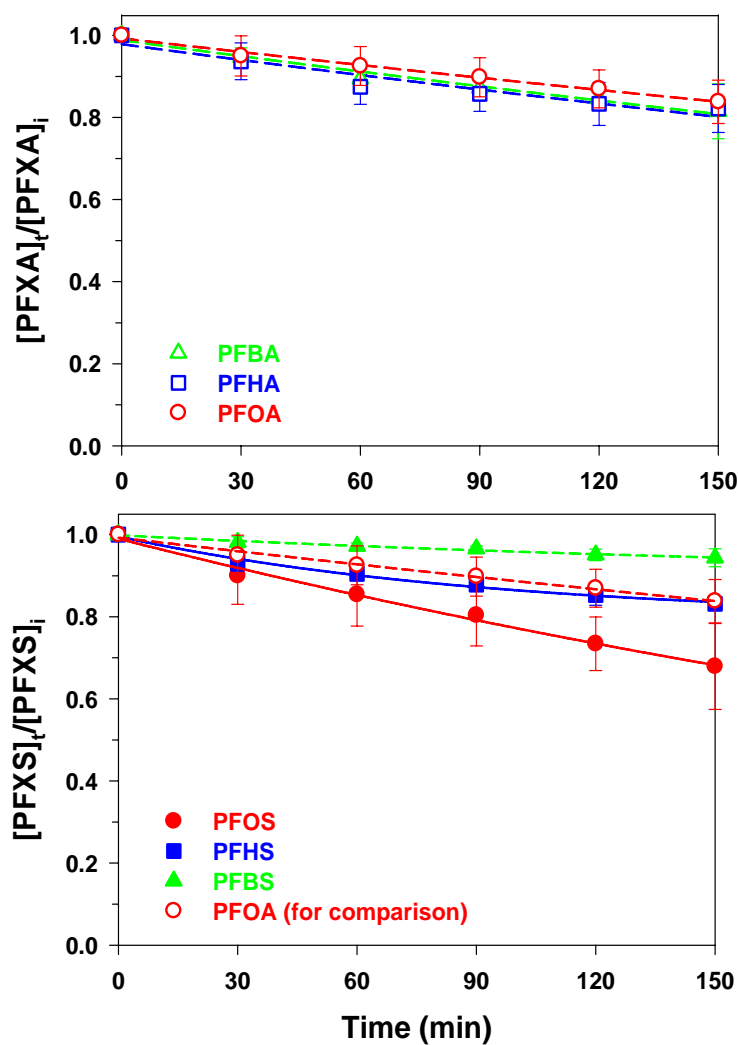




**Figure 5.4.**  $F^-$  production during PFXA and PFXS ( $X = O, H, B$ ) UV-KI photolysis. A) PFXA ( $X = O, H, B$ ), and B) PFXS ( $X = O, H, B$ ) photolysis. Experimental conditions are identical to those of Figure 5.3

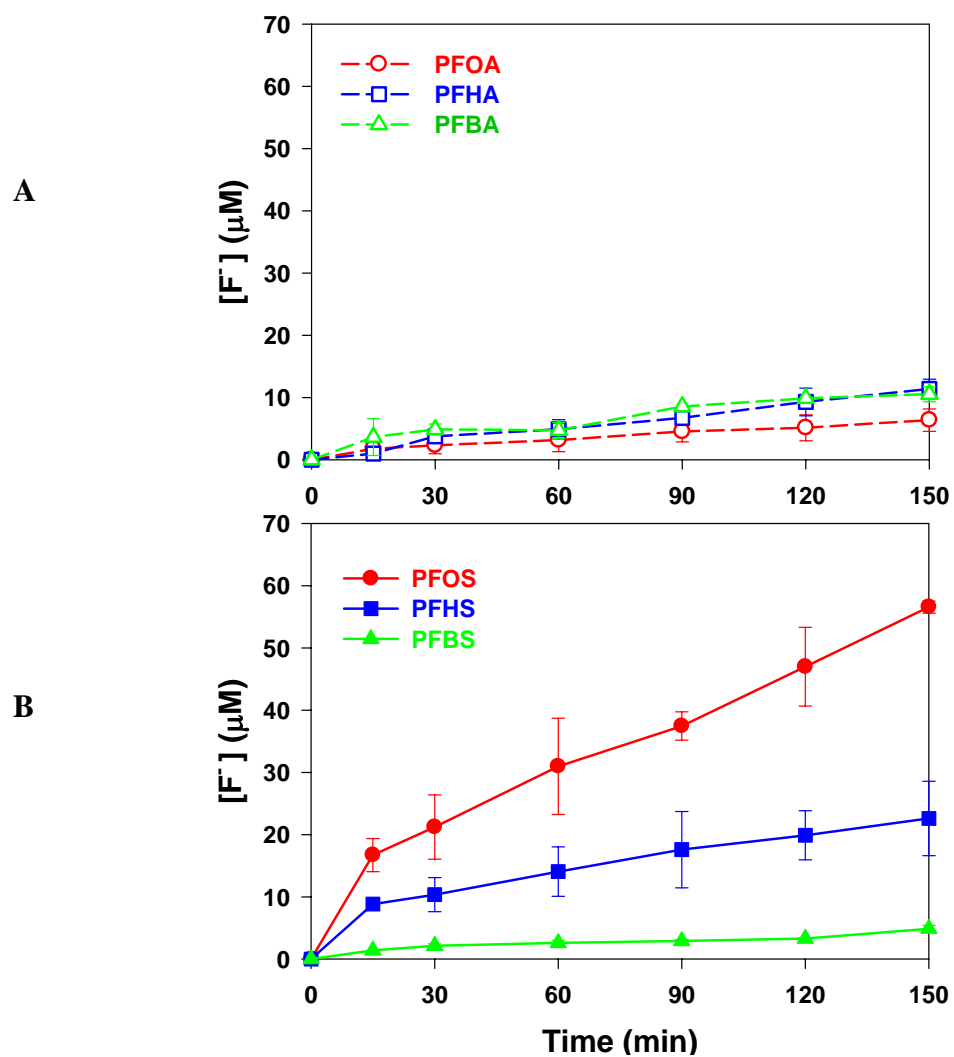


**Figure 5.5.** Effects of chain length on FC UV-KI degradation rates and F-index.

Experimental conditions are identical to those of Figure 5.3

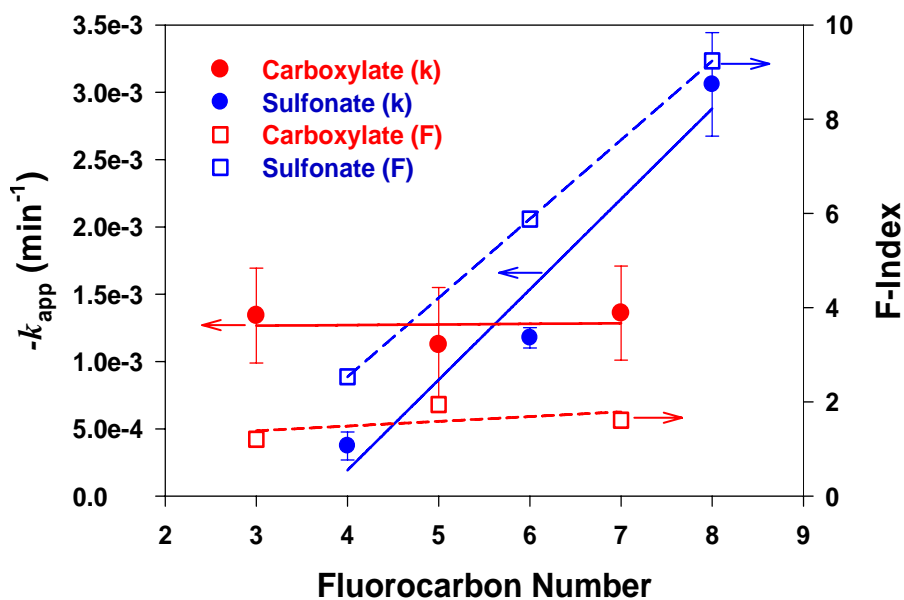
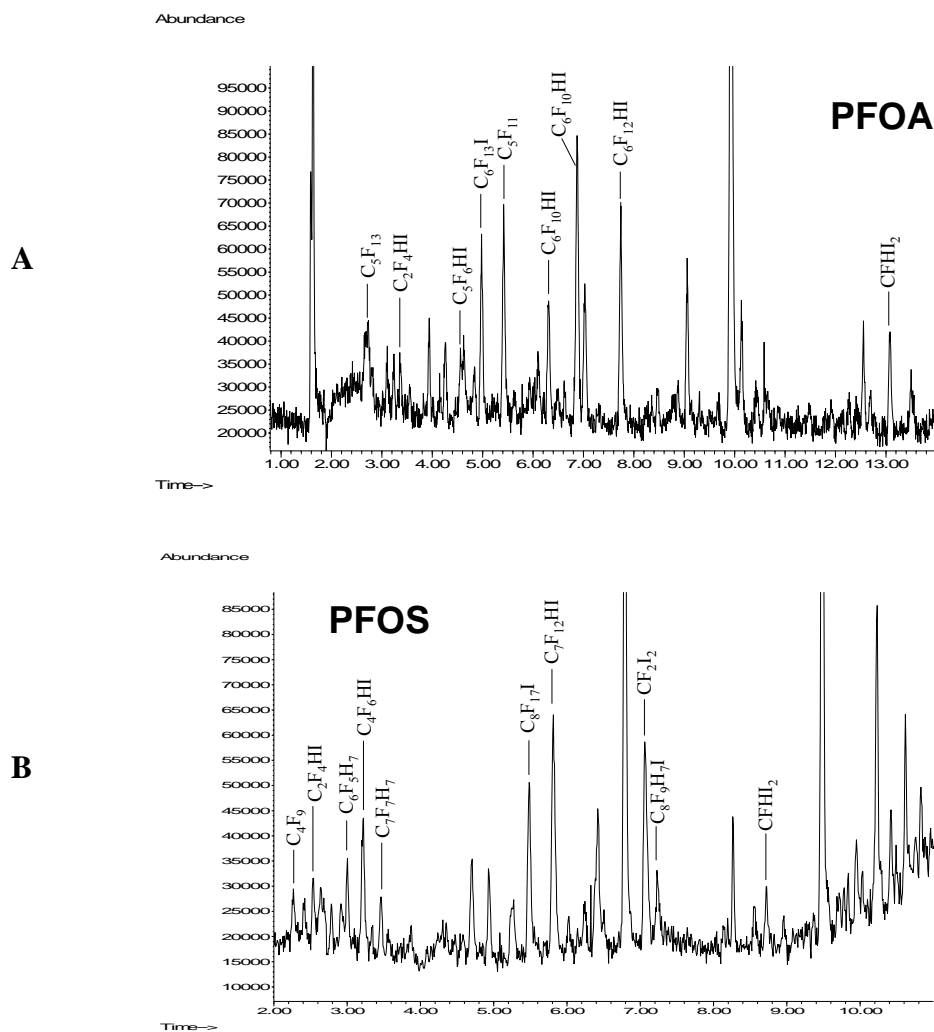


**Figure 5.6.** Gaseous products during PFOX UV-KI photolysis. Experimental conditions identical to those of Figure 5.3. A) Representative PFOA GC-MS Spectrum, B) Representative PFOS GC-MS



## Tables

**Table 5.1.** Fluorochemical UV-KI photolysis kinetics and F-index. Apparent first-order rate constants, quantum yields, and F-indexes for the decomposition of perfluoroalkylcarboxylates and perfluoroalkylsulfonates by aqueous iodide photolysis<sup>a</sup>

PFC	Formula	k (min <sup>-1</sup> )	QY	F-Index <sup>b</sup>
PFBA	CF <sub>3</sub> (CF <sub>2</sub> ) <sub>2</sub> CO <sub>2</sub> <sup>-</sup>	1.3×10 <sup>-3</sup>	7.1×10 <sup>-4</sup>	1.2
PFHA	CF <sub>3</sub> (CF <sub>2</sub> ) <sub>4</sub> CO <sub>2</sub> <sup>-</sup>	1.1×10 <sup>-3</sup>	6.9×10 <sup>-4</sup>	1.9
PFOA	CF <sub>3</sub> (CF <sub>2</sub> ) <sub>6</sub> CO <sub>2</sub> <sup>-</sup>	1.4×10 <sup>-3</sup>	6.4×10 <sup>-4</sup>	1.6
PFBS	CF <sub>3</sub> (CF <sub>2</sub> ) <sub>3</sub> SO <sub>3</sub> <sup>-</sup>	4.0×10 <sup>-4</sup>	2.4×10 <sup>-4</sup>	2.5
PFHS	CF <sub>3</sub> (CF <sub>2</sub> ) <sub>5</sub> SO <sub>3</sub> <sup>-</sup>	1.2×10 <sup>-3</sup>	5.7×10 <sup>-4</sup>	5.9
PFOS	CF <sub>3</sub> (CF <sub>2</sub> ) <sub>7</sub> SO <sub>3</sub> <sup>-</sup>	3.0×10 <sup>-3</sup>	1.2×10 <sup>-3</sup>	9.2

a) See Figure 5.3 for detailed experimental conditions.

b)  $-[F^-]_{\text{Produced}}/[PFC^-]_{\text{Degraded}}$

**Table 5.2.** Gaseous products during fluorochemical UV-KI photolysis. The gases are separated by carbon number and iodation

#C	PFBS $C_4F_9SO_3^-$		PFHS $C_6F_{13}SO_3^-$		PFOS $C_8F_{17}SO_3^-$	
	Iodide	Non-Iodide	Iodide	Non-Iodide	Iodide	Non-Iodide
8					C8F17I C8F9H8I C8F9H7I C8F6H3I C7F12HI C7F9H6I	C8F13H4 C8F13H3
7						C7F7H7 C7F6H9 C7F4H10 C6F5H7
6			C6F13I C6F12HI C6F3H8I	C6F7H5 C6F5H5		
5			C5F8HI C5F6HI C5F4H4I2 C5FH4I	C5F2H8	C5F7H2I C5F3HI	
4		C4F4H4	C4F6H3I C4F6HI C4F5H2I	C4F4H4	C4F6HI C4F5H2I C4H9I	C4F9 C4F4H2
3	C3F2I2 C3F2I C3FH2I C3FHI		C3F6HI		C3F6HI C3F4H3I	
2	C2FI C2H5I	C2F3H3	C2F4I2 C2F3H2I C2H5I C2H4I		C2F4HI C2F3HI2 C2H4I2 C2H3I2 C2H2I2 C2H5I	
1	CH2I2 CH3I		CF2I2 CH3I		CF2I2 CFHI2 CH2I2 CH3I	

#C	PFBA $C_3F_7CO_2^-$		PFHA $C_5F_{11}CO_2^-$		PFOA $C_7F_{15}CO_2^-$	
	Iodide	Non-Iodide	Iodide	Non-Iodide	Iodide	Non-Iodide
8						
7						
6					C6F13I C6F12HI C6F10HI C5F6HI	C6F5H7
5						C5F13 C5F11
4			C4F9I			
3	C3F6HI			C3F9 C3F7		
2	C2F5I C2F4I2 C2F4HI C2H6I				C2F4HI	
1	CH3I		CFHI2 CH3I CH2I2		CFHI2 CH3I CH2I2	

## References

- (1) D'Eon, J. C.; Hurley, M. D.; Wallington, T. J.; Mabury, S. A. *Environ. Sci. Technol.* **2006**, *40*, 1862.
- (2) Martin, J. W.; Ellis, D. A.; Mabury, S. A.; Hurley, M. D.; Wallington, T. J. *Environ. Sci. Technol.* **2006**, *40*, 864.
- (3) Xu, L.; Krenitsky, D. M.; Seacat, A. M.; Butenhoff, J. L.; Anders, M. W. *Chem. Res. Toxicol.* **2004**, *17*, 767.
- (4) Tomy, G. T.; Tittlemier, S. A.; Palace, V. P.; Budakowski, W. R.; Braekevelt, E.; Brinkworth, L.; Friesen, K. *Environ. Sci. Technol.* **2004**, *38*, 758.
- (5) Scott, B. F.; Moody, C. A.; Spencer, C.; Small, J. M.; Muir, D. C. G.; Mabury, S. A. *Environ. Sci. Technol.* **2006**, *40*, 6405.
- (6) Skutlarek, D.; Exner, M.; Farber, H. *Environ. Sci. Pollut. Res.* **2006**, *13*, 299.
- (7) Shoeib, M.; Harner, T.; Vlahos, P. *Environ. Sci. Technol.* **2006**, *40*, 7577.
- (8) Yamashita, N.; Kannan, K.; Taniyasu, S.; Horii, Y.; Petrick, G.; Gamo, T. *Mar. Pollut. Bull.* **2005**, *51*, 658.
- (9) The Science of Organic Fluorochemistry. Office of Pollution Prevention and Toxics; Docket AR226-0547; U.S. Environmental Protection Agency: Washington, D.C., 1999; p. 12.
- (10) Schroder, H. F.; Meesters, R. J. W. *J. Chromatogr. A* **2005**, *1082*, 110.
- (11) Dillert, R.; Bahnemann, D.; Hidaka, H. *Chemosphere* **2007**, *67*, 785.
- (12) Hori, H.; Hayakawa, E.; Einaga, H.; Kutsuna, S.; Koike, K.; Ibusuki, T.; Kiatagawa, H.; Arakawa, R. *Environ. Sci. Technol.* **2004**, *38*, 6118.

- (13) Hori, H.; Yamamoto, A.; Hayakawa, E.; Taniyasu, S.; Yamashita, N.; Kutsuna, S. *Environ. Sci. Technol.* **2005**, *39*, 2383.
- (14) Wardman, P. *J. Phys. Chem. Ref. Data* **1989**, *18*, 1637.
- (15) Buxton, G. V.; Greenstock, C. L.; Helman, W. P.; Ross, A. B. *J. Phys. Chem. Ref. Data* **1988**, *17*, 513.
- (16) Szajdzinska-Pietek, E.; Gebicki, J. L. *Res. Chem. Intermed.* **2000**, *26*, 897.
- (17) Moriwaki, H.; Takagi, Y.; Tanaka, M.; Tsuruho, K.; Okitsu, K.; Maeda, Y. *Environ. Sci. Technol.* **2005**, *39*, 3388.
- (18) Vecitis, C. D.; Park, H.; Cheng, J.; Mader, B. T.; Hoffmann, M. R. *J. Phys. Chem. A* **2008**, *112*, 4261.
- (19) Kutsuna, S.; Hori, H. *Int. J. Chem. Kinet.* **2007**, *39*, 276.
- (20) Huang, L.; Dong, W. B.; Hou, H. Q. *Chem. Phys. Lett.* **2007**, *436*, 124.
- (21) Neta, P.; Huie, R. E.; Ross, A. B. *J. Phys. Chem. Ref. Data* **1988**, *17*, 1027.
- (22) Yamamoto, T.; Noma, Y.; Sakai, S. I.; Shibata, Y. *Environ. Sci. Technol.* **2007**, *41*, 5660.
- (23) Hori, H.; Nagaoka, Y.; Yamamoto, A.; Sano, T.; Yamashita, N.; Taniyasu, S.; Kutsuna, S.; Osaka, I.; Arakawa, R. *Environ. Sci. Technol.* **2006**, *40*, 1049.
- (24) Hori, H.; Nagaoka, Y.; Sano, T.; Kutsuna, S. *Chemosphere* **2008**, *70*, 800.
- (25) Shoute, L. C. T.; Mittal, J. P.; Neta, P. *J. Phys. Chem.* **1996**, *100*, 3016.
- (26) Shoute, L. C. T.; Mittal, J. P.; Neta, P. *J. Phys. Chem.* **1996**, *100*, 11355.
- (27) Combellas, C.; Kanoufi, F.; Thiebault, A. *J. Phys. Chem. B* **2003**, *107*, 10894.
- (28) Corvaja, C.; Farnia, G.; Formenton, G.; Navarrini, W.; Sandona, G.; Tortelli, V. *Journal of Physical Chemistry* **1994**, *98*, 2307.

- (29) Watson, P. L.; Tulip, T. H.; Williams, I. *Organometallics* **1990**, 9, 1999.
- (30) Burdeniuc, J.; Chupka, W.; Crabtree, R. H. *J. Am. Chem. Soc.* **1995**, 117, 10119.
- (31) Macnicol, D. D.; Robertson, C. D. *Nature* **1988**, 332, 59.
- (32) Scherer, K. V.; Ono, T.; Yamanouchi, K.; Fernandez, R.; Henderson, P.; Goldwhite, H. *J. Am. Chem. Soc.* **1985**, 107, 718.
- (33) Anbar, M.; Hart, E. J. *J. Phys. Chem.* **1965**, 69, 271.
- (34) Pud, A. A.; Shapoval, G. S.; Kukhar, V. P.; Mikulina, O. E.; Gervits, L. L. *Electrochim. Acta* **1995**, 40, 1157.
- (35) Marsella, J. A.; Gilicinski, A. G.; Coughlin, A. M.; Pez, G. P. *J. Org. Chem.* **1992**, 57, 2856.
- (36) Chen, X. D.; Lemal, D. M. *J. Fluor. Chem.* **2006**, 127, 1158.
- (37) Ono, T.; Fukaya, H.; Hayashi, E.; Saida, H.; Abe, T.; Henderson, P. B.; Fernandez, R. E.; Scherer, K. V. *J. Fluor. Chem.* **1999**, 97, 173.
- (38) Rahn, R. O.; Stephan, M. I.; Bolton, J. R.; Goren, E.; Shaw, P.-S.; Lykke, K. R. *Photochem. Photobiol.* **2003**, 78, 146.
- (39) Sauer, M. C.; Crowell, R. A.; Shkrob, I. A. *J. Phys. Chem. A* **2004**, 108, 5490.
- (40) Lehr, L.; Zanni, M. T.; Frischkorn, C.; Weinkauff, R.; Neumark, D. M. *Science* **1999**, 284, 635.
- (41) Andrieux, C. P.; Combella, C.; Kanoufi, F.; Saveant, J. M.; Thiebault, A. *J. Am. Chem. Soc.* **1997**, 119, 9527.
- (42) Avila, D. V.; Ingold, K. U.; Lusztyk, J.; Dolbier, W. R.; Pan, H. Q. *J. Am. Chem. Soc.* **1993**, 115, 1577.



- (43) Avila, D. V.; Ingold, K. U.; Lusztyk, J.; Dolbier, W. R.; Pan, H. Q.; Muir, M. J. *Am. Chem. Soc.* **1994**, *116*, 99.
- (44) Zhang, L.; Dolbier, W. R.; Sheeller, B.; Ingold, K. U. *J. Am. Chem. Soc.* **2002**, *124*, 6362.
- (45) Dolbier, W. R. *Chem. Rev.* **1996**, *96*, 1557.
- (46) Hart, E. J.; Anbar, M. *The Hydrated Electron*; Wiley-Interscience: New York, 1970.